JOURNAL OF GEOPHYSICAL RESEARCH, VOL. 113, D16106, doi:10.1029/2007JD008915, 2008

Geomagnetic perturbations on stratospheric circulation in late winter and spring

Hua Lu,[1] Mark A. Clilverd,[1] Annika Seppälä,[1,2] and Lon L. Hood[3]

Received 4 May 2007; revised 4 June 2008; accepted 11 June 2008; published 22 August 2008.

[1] This study investigates if the descent of odd nitrogen, generated in the thermosphere and the upper mesosphere by energetic particle precipitation (EPP-NO_x), has a detectable impact on stratospheric wind and temperature in late winter and spring presumably through the loss of ozone and reduction of absorption of solar UV. In both hemispheres, similar downward propagating geomagnetic signals in the extratropical stratosphere are found in spring for those years when no stratospheric sudden warming occurred in mid-winter. Anomalous easterly winds and warmer polar regions are found when the 4-month averaged winter Ap index (A_p) is high, and the signals become clearer when solar F10.7 is low. In May, significant geomagnetic signals are obtained in the Northern Hemisphere when the data are grouped according to the phase of the stratospheric equatorial QBO. The magnitudes of changes in spring stratospheric wind and temperatures associated with A_p signals are in the range of 10–20 m s^{-1} and 5–10 K, which are comparable with those of the 11-yr SC signals typically found in late winter. The spring A_p signals show the opposite sign to that expected due to *in situ* cooling effects caused by catalytic destruction of stratospheric ozone by descending EPP-NO_x. Thus it is unlikely that the *in situ* chemical effect of descending EPP-NO_x on stratospheric ozone would have a dominant influence on stratospheric circulation. Instead, we suggest that the detected A_p signals in the extratropical spring stratosphere may be an indirect consequence of geomagnetic and solar activity, dynamically induced by changes in wave ducting conditions.

Citation: Lu, H., M. A. Clilverd, A. Seppälä, and L. L. Hood (2008), Geomagnetic perturbations on stratospheric circulation in late winter and spring, *J. Geophys. Res.*, *113*, D16106, doi:10.1029/2007JD008915.

1. Introduction

[2] There is growing evidence that the Sun may affect Earth's climate by multiple means. Apart from well reported correlations between the 11-year solar cycle (11-yr SC) and atmospheric temperature [*Labitzke and van Loon*, 2000; *Crooks and Gray*, 2005], statistical correlations have been established between geomagnetic activity and atmospheric variables such as the North Atlantic Oscillation (NAO) and geopotential height [*Thejll et al.*, 2003; *Bochnicek and Hejda*, 2005]. *Boberg and Lundstedt* [2002, 2003] found that the variation of the winter NAO index is correlated with the electric field strength of the solar wind, and suggested a solar wind generated electromagnetic disturbance in the ionosphere may dynamically propagate downward through the atmosphere. GCM studies have suggested that the stratospheric temperature response to the enhancement of solar wind driven magnetic flux is through the coupling of changes in atmospheric mean flow and planetary waves [*Arnold and Robinson*, 2001]. The solar wind may also induce heating in the middle stratosphere and thus influence atmospheric circulation [*Zubov et al.*, 2005].

[3] The physical processes by which the effects of geomagnetic variability may propagate to the lower atmosphere are yet to be understood. One possible mechanism of downward transfer of geomagnetic influences is through energy deposition and changes in chemical constituents via energetic particle precipitation (EPP), which may potentially influence the atmospheric circulation through dynamical–chemical coupling [*Solomon et al.*, 1982]. EPP leads to production of odd nitrogen NO_x ($NO + NO_2$) in the mesosphere and the lower thermosphere, and to sporadic NO_x production in the stratosphere via high-energy particle precipitation. During polar winter and spring, the EPP induced NO_x (EPP-NO_x) may descend into the upper stratosphere, perturbing stratospheric ozone (O_3) chemistry through catalytic reactions, which in turn will affect the stratospheric radiative balance and thus may affect the circulation [*Brasseur and Solomon*, 2005].

[4] Although the recent observational studies have established an apparent linkage between descending polar NO_x and upper stratospheric O_3 depletions [*Randall et al.*, 2005; *Clilverd et al.*, 2006; *Hauchecorne et al.*, 2007; *Seppälä et al.*, 2007], the net impact of EPP-NO_x on stratospheric O_3 and the consequent effects on the stratospheric circulation

[1]Physical Sciences Division, British Antarctic Survey, Cambridge, UK.
[2]Earth Observation, Finnish Meteorological Institute, Helsinki, Finland.
[3]Lunar and Planetary Laboratory, University of Arizona, Tuczon, Arizona, USA.

0148-0227/08/2007JD008915

remain poorly quantified. A major difficulty is that the production altitude of NO_x depends on the energy spectrum of the particles and thus the stratospheric NO_x enhancement can originate from a wide range of processes [*Seppälä et al.*, 2007]. Impulsive episodes of Solar Proton Events (SPEs) which are rather sporadic and are able to directly penetrate into the stratosphere to generate stratospheric NO_x *in situ*, should be considered as a additional cause of stratospheric high-latitude NO_x [*Jackman and McPeters*, 2004]. High-energy relativistic electron precipitation (REP) produces NO_x in the high latitude mesosphere at altitudes of $\sim$60–80 km, and tends to peak around solar minimum [*Callis et al.*, 1991, 2001]. Medium-energy auroral EPP, which peaks preferentially in the descending phase of the 11-yr SC [*Vennerstrøm and Friis-Christensen*, 1996], produces NO_x routinely in the mesosphere and the thermosphere ($\sim$90–120 km) [*Brasseur and Solomon*, 2005]. Also, galactic cosmic rays that peak at solar minimum can lead to secondary NO_x production in the lower stratosphere.

[5] A few modeling studies have been undertaken to understand stratospheric responses to the NO_x enhancement. As different assumptions have been made for different models, the modeled temperature responses differ widely from one model to another in both magnitude and spatial patterns. By using the Whole Atmosphere Community Climate Model (WACCM3), *Jackman et al.* [2008] predicted >20% O_3 loss in the polar middle to upper stratosphere due to downward transport of induced NO_x following extremely large SPEs. For the well-documented SPEs during October–November 2003 (4th largest since 1963), it was estimated that 10–60% O_3 depletion lasted days beyond the events in the polar upper stratosphere and 1–10% O_3 loss lasted for a few months [*Seppälä et al.*, 2004; *Jackman et al.*, 2005]. Using the Thermosphere Ionosphere Mesosphere Electrodynamics-GCM (TIME-GCM), *Jackman et al.* [2007] further showed that temperature changes associated with 2003 SPEs were mainly concentrated in the sunlit Southern Hemisphere (SH) mesosphere as temperature changes in the winter hemisphere would be small due to the lack of sunlight to be absorbed by the O_3. The O_3 loss led to up to 2.6 K decreases in zonal-mean temperature in the high latitude middle mesosphere, while modest temperature increases (<1 K, <1%) were found in the stratosphere. *Rozanov et al.* [2005] studied REP induced NO_y(= NO_x + NO_3 + HNO_3 + $ClNO_3$ + $2N_2O_5$ + HNO_4) during 1987, a year with relatively low geomagnetic activity, on stratospheric O_3 and temperature using a 3D chemistry-climate model. They found that REP induced NO_y led to 3–5% of annual O_3 loss outside the polar stratosphere and up to 30% in the polar latitudes with higher O_3 loss occurring during spring. Mean annual temperature was predicted to decrease by up to 1 K in the upper and middle stratosphere outside the polar latitudes, and up to 5 K in the SH polar latitudes. An intensification of the polar vortex and small perturbations to the surface air temperature were also predicted. They concluded that the magnitude of the atmospheric response to the EPP could exceed the effects from varying solar UV flux.

[6] *Langematz et al.* [2005] also modeled atmospheric responses to REP by using the Freie Universität Berlin Climate Middle Atmosphere Model with interactive chemistry (FUB-CMAM-CHEM). They found that doubling the NO_x source in the polar region between 73 and 84 km at solar minimum led to 40–50% less O_3 throughout the polar stratosphere and 30–40% less O_3 in the lower equatorial stratosphere between solar maximum and solar minimum. *Marsh et al.* [2007] used WACCM3 to simulate 11-yr SC influences on the atmospheric circulation by imposing a higher geomagnetic Ap index (i.e., increased NO production in the thermosphere) under solar maximum. They found that effects on stratospheric O_3 via downward transport of thermospheric NO are indirect in the polar middle and upper stratosphere. The estimated changes associated with O_3 and temperature are at least one order of magnitude smaller than those reported by *Rozanov et al.* [2005] and *Langematz et al.* [2005].

[7] By using homogeneous radiosonde measurements over 1968–2004 and from the surface to 30 hPa ($\sim$23 km altitude), the statistical inferences of *Lu et al.* [2007] reported positive temperature responses to the geomagnetic Ap index in the high-latitude Northern Hemisphere (NH) lower stratosphere when the data were treated by filtering out the periods shorter than 12 months. The authors reported up to 0.6 K increases in the temperature anomalies in the Arctic lower stratosphere, though the filtering window was too long to detect a seasonal distribution. They also found that those positive geomagnetic activity signatures in the NH polar annual temperature were preferably associated with low solar activity. They suggested that those geomagnetic signals are likely due to indirect or dynamical responses instead of *in situ* cooling caused by O_3 depletion by EPP-NO_x. The GCM modeling study of *Arnold and Robinson* [1998] showed that planetary waves can couple solar-induced changes in the thermosphere down to the stratosphere. They demonstrated that, in the winter hemisphere, the 11-yr SC modulation of planetary wave propagation reinforces small but persistent perturbations in the thermosphere. This leads to changes in middle atmosphere circulation with a significantly weakened winter stratospheric vortex under high solar activity. *Arnold and Robinson* [2001] extended this work to show that geomagnetic variability could produce a similar stratospheric response when no stratospheric *in situ* forcing, such as that associated with increases in solar ultraviolet (UV) irradiance, was applied.

[8] The current literature suggests that the route by which geomagnetic variability might affect climate remains a provocative question that warrants further examination. The modeled stratospheric temperature responses to NO_x enhancement include both direct and localized heating and cooling caused by photochemical reactions, and indirect and nonlocal responses to changes induced by atmospheric dynamical conditions. It remains unclear whether or not EPP-NO_x plays a major role in the variability of stratospheric O_3 and circulation, and whether the *in situ* or nonlocal mechanism dominates. Questions also remain about if and how changes occurring in the upper atmosphere could interact with upward propagating waves, and consequently alter the dynamical condition of the stratosphere.

[9] This study makes a statistical assessment of possible geomagnetic activity influences on atmospheric circulation on a month-by-month basis. By using the longest possible atmospheric reanalysis data set available, we aim to address three research questions: 1) Can we detect geomagnetic Ap

signals in stratospheric dynamical variables in late winter and spring? 2) Does geomagnetic variability affect the extratropical stratosphere primarily through the mechanism of the descending EPP-NO_x? 3) Are atmospheric responses to geomagnetic activity modulated by the 11-yr SC or the QBO?

2. Data and Methods

[10] After sunset, chemical processes within the NO_x family lead to rapid conversion of NO to NO_2. Hence nighttime NO_2 measurements represent the overall levels of NO_x reasonably well. Vertical profiles of several chemical species including NO_2 (20–50/70 km) and O_3 (10–100 km) have been retrieved from the Global Ozone Monitoring by Occultation of Stars (GOMOS) instrument on board the Envisat satellite since 2002 [*Bertaux et al.*, 2000; *Kyrölä et al.*, 2004; *Hauchecorne et al.*, 2005, 2007]. The stellar occultation technique allows NO_2 measurements to be made in the dark wintertime polar latitudes. Nighttime GOMOS (GOPR version 6.0f) NO_2 measurements are presented here to show the descent of NO_x in the polar region and its possible relation to geomagnetic activity. The measurement selection criteria are the same as that of *Seppälä et al.* [2007]. The analysis is further complemented with measurements made by SAGE III (version 3, sunset events, available at http://eosweb.larc.nasa.gov) and POAM III (version 4, available at http://wvms.nrl.navy.mil). Both SAGE III and POAM III instruments use the solar occultation technique and are thus unable to make measurements in the polar night region [*Randall et al.*, 2002]. As the GOMOS measurements represent nighttime NO_2 while POAM/SAGE data represent the daytime NO_2, there is an expected difference between the amount of NO_2 observed by GOMOS and SAGE/POAM. This is due to the diurnal variation of NO_2, reflecting the differences in the day and nighttime NO_x partitioning.

[11] The atmospheric data used here are monthly-mean zonal wind and temperatures from ECMWF (European Centre for Medium Range Weather Forecasting) ERA-40 Reanalysis (September 1957 to August 2002) and ECMWF Operational analyses (September 2002 to December 2006). The ERA-40 Reanalysis has a spectral resolution of T159, corresponding to a 1.125° horizontal resolution in latitude and longitude. The data are available at 23 standard pressure surfaces from 1000 hPa to 1 hPa, which were assimilated using direct radiosonde and satellite measurements [*Uppala et al.*, 2005]. The ECMWF Operational data were output from the ongoing analyses produced by the most recent ECMWF Integrated Forecasting System (IFS) model. Data from September 2002 to the present day are available on the same 1.125° grid and 21 pressure levels, which are identical to the ERA-40 data except without the 600 and 775 hPa levels. Data below 300 hPa are excluded from this study so those missing levels have no effect here. It is known that larger uncertainty in the ERA-40 reanalysis exists in the SH than in the NH. The scarcity of SH radiosonde measurements results in unreliable estimations before the satellite era (i.e., pre-1979) due to poorly constrained model output. For this reason, we use the full data length for the NH but data since 1979 for the SH.

[12] The Ap index is a measure of the global levels of geomagnetic disturbance [*Mayaud*, 1980], and is a good proxy for the energy deposited in the Earth's upper atmosphere by EPP [*Siskind et al.*, 2000]. The monthly averaged Ap index ranges typically from 4–44, and 4-month averages range from 6 to 30 for the period of 1958–2006. Low Ap values indicate a quiescent interplanetary medium as well as low solar wind speed [*Garrett et al.*, 1974]. We obtain the monthly averaged Ap index from the National Geophysical Data Center (NGDC) website (www.ncdc.noaa.gov/stp). The 10.7-cm solar radio flux data (F10.7) are also downloaded from the NGDC website and are used here to represent variations of solar irradiance over the 11-yr SC.

[13] A list of major sudden stratospheric warming (SSW) events over the period of 1958–2001 was compiled by *Charlton and Polvani* [2007]. It is used here to identify those years when the NH polar vortex was dynamically disrupted during the middle to late winter. Excluding those years affected by the major SSWs may provide a statistically more suitable condition for EPP-NO_x to descend into the lower atmosphere [*Randall et al.*, 2005]. Similarly, data for 2002 are excluded from the SH analyses to account for the unprecedented major SSW event which occurred in September 2002. To avoid contamination by the warming caused by volcanic aerosols in the stratosphere, two years of data following three major eruptions (i.e., Agung in March, 1963, El Chichón in April, 1982, and Pinatubo in June, 1991) are also excluded from our analysis.

[14] The main diagnostic tools employed are composite analysis and linear correlation. The significance of the correlations is tested by using the method of *Davis* [1976], which is based on the concept of Effective Sample Size (ESS). The same Monte Carlo significance test used by *Lu et al.* [2007] is used to test the statistical significance of the composite differences.

3. Observations of Descending NO_x

[15] In this Section, we summarize the essential features of EPP-NO_x using satellite observations. These features will help us to set up a benchmark that facilitates a comparison with the geomagnetic signals found in the stratospheric wind and temperature. The upper panels of Figure 1 show GOMOS and SAGE III observations of descending NO_x in the NH winter/spring (December 2003–May 2004, left) and GOMOS and POAM III observations in the SH winter/spring (May–October, 2003, right). These two winters were chosen as examples of significant NO_x descent events that have taken place in recent years. The plots show the NO_2 mixing ratio from 30–70 km. Above these altitudes the chemical lifetime of NO_2 is short and the abundance too low for NO_2 to be detectable to the satellite instruments and thus the NO_2 measurements are no longer available for the approximation of the nighttime NO_x, although EPP-NO_x can be detected at altitudes of 70–90 km by radio propagation techniques [*Clilverd et al.*, 2006]. The transition from GOMOS to SAGE III data in the NH panel occurs at the end of February when GOMOS nighttime measurements in the Arctic end. In the SH panel POAM III data are also used to supplement GOMOS data gaps. Note that different NO_x mixing ratio color scales are used for the GOMOS, SAGE

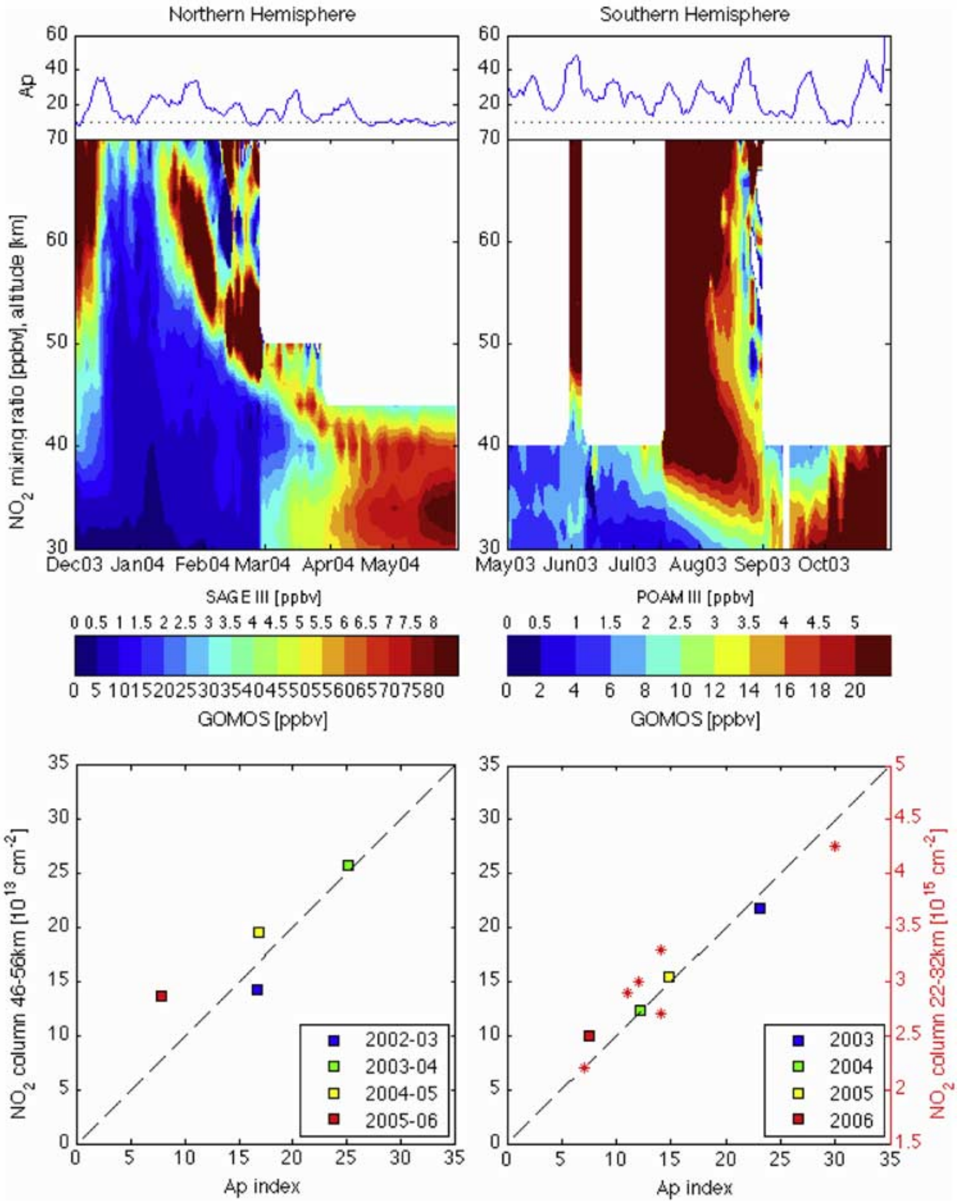

Figure 1. (top row) GOMOS (data for 30–70 km, nighttime NO_2) and SAGE III (data for 30–50 km, sunset NO_2) observations of descending NO_2 in the NH winter/spring (left panel, December 2003–May 2004) and GOMOS (data for 30–70 km) and POAM III (data for 30–40 km, sunset NO_2) observations in the SH winter/spring (right panel, May 2003–October 2003). The NO_2 values have been averaged over two days. The panels show the NO_2 mixing ratio from 30 to 70 km and in the latitude range of 60°–90° with the time series of 7-day running mean Ap for the periods of interest shown above. The SAGE and POAM measurements are shown simply to indicate the progress of the descent. NO_2 has a strong diurnal variation and therefore we have adopted different color scales for the different measurements. (bottom row). The column density of NO_2 between 46 and 56 km in both the NH (left panel, October–January) and the SH (right panel, May–August), for each winter/spring since 2002 using GOMOS data, plotted against the 4-month average A_p index (A_p) [from *Seppälä et al.*, 2007]. Additional data points in red taken from *Siskind* [2000] show NO_2 column density at altitudes 22–32 km in the SH.

III and POAM III, in order to maximize the details of the NO_2 descent.

[16] In the event shown in the upper panels of Figure 1, the descent of NO_2 takes up to four months in both hemispheres. The lowest altitude that the NO_x enhancement reaches in the NH is ~40 km, while in the SH it is noticeably lower, at ~30 km. At the lowest altitudes, the NO_x persists for another month or so before the NO_2 enhancement features become indistinct. The lower panels of Figure 1 show the column density of NO_2 between 46–56 km in both the NH (left) and SH (right), for each winter/spring since 2002 estimated using GOMOS measurements

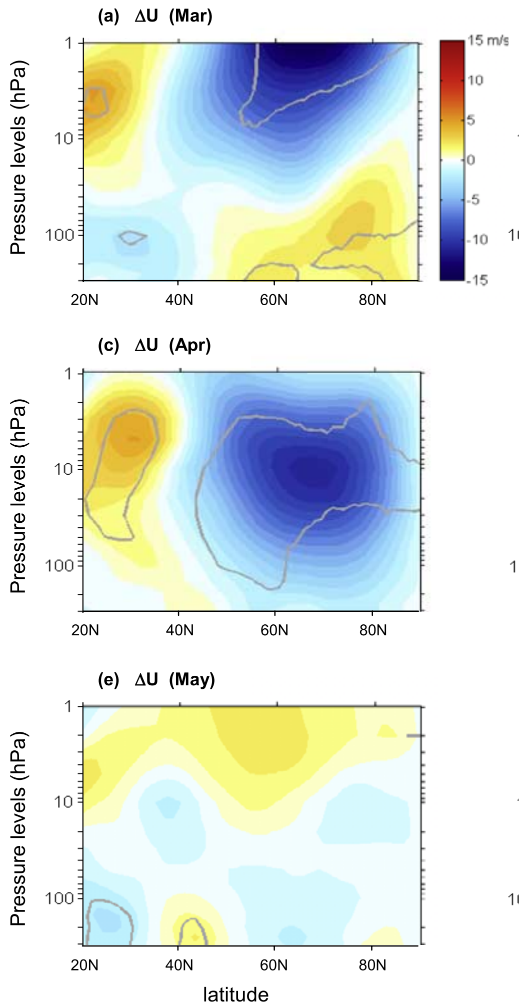

Figure 2. Composite differences between HG and LG for zonal-mean zonal wind ΔU (m s^{-1}, left-hand panels) and for temperature ΔT (K, right-hand panels) for the months from March to May (top to bottom), displayed in the NH meridional-vertical cross section. The years in which a major SSW occurred or affected by a major volcanic eruption are excluded, and the data are grouped into $\geq$ and < median(A_p), where A_p is the 4-month averaged Ap index with Nov–Feb, Dec–Mar and January–April mean for March, April and May, respectively, for March to May analyses. The areas enclosed within the grey lines indicate that the differences are statistically significant from zero with a confidence level of 90% or above, calculated using a Monte Carlo trial based non-parametric test.

only, plotted against the 4-month average Ap index (A_p) [*Seppälä et al.*, 2007]. The SH panel also shows the NO_2 column density for ~22–32 km in red stars from *Siskind et al.* [2000] during 1991–1996. The months used in producing the NO_2 column and the A_p were: October–January for the NH, and May–August for the SH. The panels show that similar amounts of NO_2 are observed in each hemisphere and that there is a nearly linear relationship between the upper stratospheric NO_2 and A_p [*Seppälä et al.*, 2007]. Note that the event of descending NO_x such as the one that occurred in 2003/2004 late winter and spring was rare in the NH, while the event shown in right-hand panel of Figure 1 were observed more regularly in the SH. In summary, the GOMOS observations suggest that, in late winter and spring and in the latitude region of 60°–90°, the NO_x is likely to reach the upper stratosphere (~40–50 km, or 3–0.5 hPa), where the average stratospheric NO_x column density is shown to be correlated to the 4-month averaged geomagnetic Ap index (referred as A_p hereinafter).

[17] In section 4, we search for the signature of the descending NO_x in atmospheric reanalysis data. We assume that EPP-NO_x will reduce stratospheric O_3 through catalytic reaction cycles and therefore decrease the *in situ* temperature and produce more westerly winds in the extratropical region. We use A_p as a proxy to account for the accumulative effects of EPP-NO_x in our statistical analyses. In order to account for the delayed stratospheric response to EPP-NO_x, a 1–3 month backward lag is applied to A_p as well. As the time series of A_p obeys a log-normal distribution, A_p greater or smaller than its median is defined as high and low geomagnetic activity, while high and low solar activity are defined by the monthly mean values of F10.7. For simplicity, hereinafter, high and low A_p are shorthanded as HG and LG, and high and low F10.7 are shorthanded as HS and

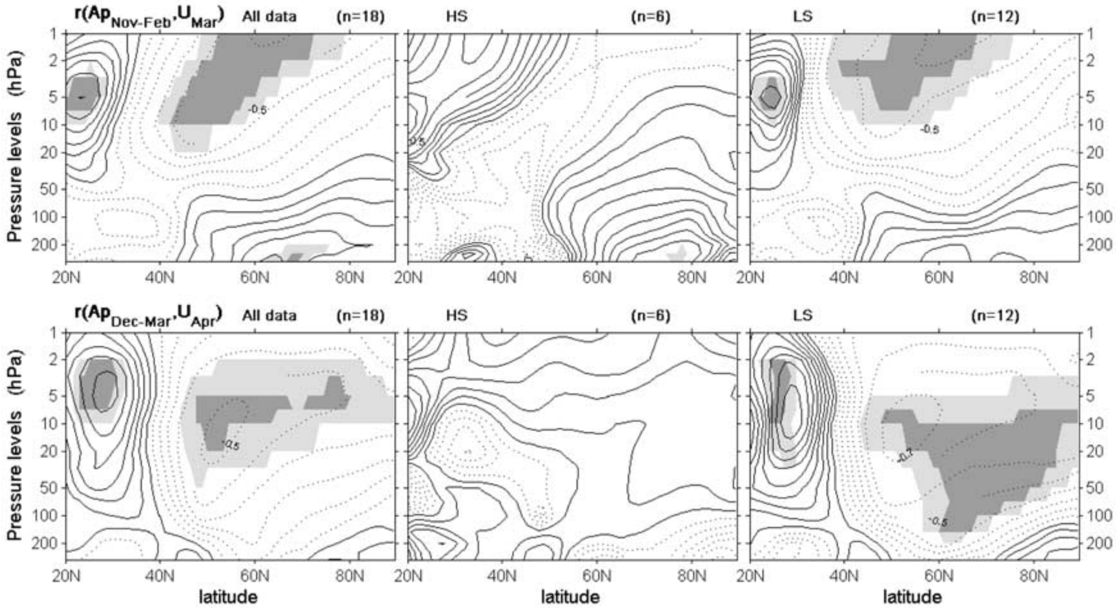

Figure 3. Correlations between $A_{p\ \mathrm{Nov-Feb}}$ and May (the 1st row), and April (the 2nd row) zonal wind, for all data (the 1st column), under HS (the 2nd column), and under LS (the 3rd column), displayed in the NH meridional-vertical cross section. The number of data points (i.e., years) used to calculate the correlation coefficients (r) are indicated on the top of each panel. The contour interval is ±0.1. Solid and dotted lines are positive and negative correlations, respectively. Shaded areas denote confidence levels above 90% (light shaded), and above 95% (dark shaded), respectively, calculated using the method of *Davis* [1976].

LS, respectively. Note that the separation of HG and LG is made by using the median value of A_p for individual calendar months rather than by that of all months. Similarly, the separation of HS and LS is made by using the mean value of F10.7 for each calendar month as well. The median values of A_p range from 12.33 for January to 15.33 for April, and the mean values of F10.7 range from 127 in December to 131 in January in the unit of solar flux units (1 sfu = 10^{-22} Wm^{-2} Hz^{-1}).

4. A_p Signatures in Zonal-Mean Zonal Wind and Temperature

[18] In this section, composite and linear correlation analyses are performed to detect geomagnetic signals in the atmospheric data for late winter and spring months. For each hemisphere, composite analyses are first performed. Linear correlation is then used to check whether similar geomagnetic signals also exist if different analytical methods are applied and whether either the 11-yr SC or the QBO modulates the geomagnetic signals.

[19] As the descent of EPP-NO_x is facilitated by confinement of descending air within the polar vortex, which deters horizontal transport to lower latitudes where EPP-NO_x would be more efficiently dissociated, a stronger, more stable polar vortex is expected to lead to more efficient downward transport of EPP-NO_x to the stratosphere [*Randall et al.*, 2005]. To maximize the chance of detecting the cooling effects due to loss of stratospheric O_3 through the catalytic NO_x cycle, we minimize the possibility of NO_x loss by excluding from our statistical analyses those years in which major SSWs occurred in middle to late winter. Effectively, we assume that there is a steady downward transport of NO_x provided that there is a stable polar vortex. This allows us to examine the stratospheric dynamical variables in relation to the production rate of EPP-NO_x in the upper mesosphere and lower thermosphere.

[20] All our analyses are performed using monthly mean of zonally averaged values for both wind and temperature, covering mid-latitude to polar stratospheric region in the meridional–vertical cross section of 20°–90°, 1–300 hPa. For either the NH or the SH, it is always possible to find A_p signals within a small confined region which are statistically significant, such "signals" are likely to have been caused by statistical fluctuations and are excluded from our report below.

4.1. A_p Signals in the NH

[21] In the NH, excluding those years in which major SSWs occurred during January to March, Figure 2 shows the composite differences of wind (left panels) and temperature (right panels) from March to May (from top to bottom) between HG and LG, which is determined by the median values of November–February, December–March, and January–April Ap index, respectively. In total, there are 18 years (1959, 1961, 1962, 1967, 1972, 1974, 1975, 1976, 1978, 1986, 1990, 1991, 1994, 1995, 1996, 1997, 1998, and 2006) in which no major SSW occurred during January to March, of those years there are 9 with HG and 9 with LG. In March, the averaged Arctic stratospheric zonal winds are up to 15 m s^{-1} less westerly under HG than under LG, while the temperature is up to 10 K warmer. Similar patterns

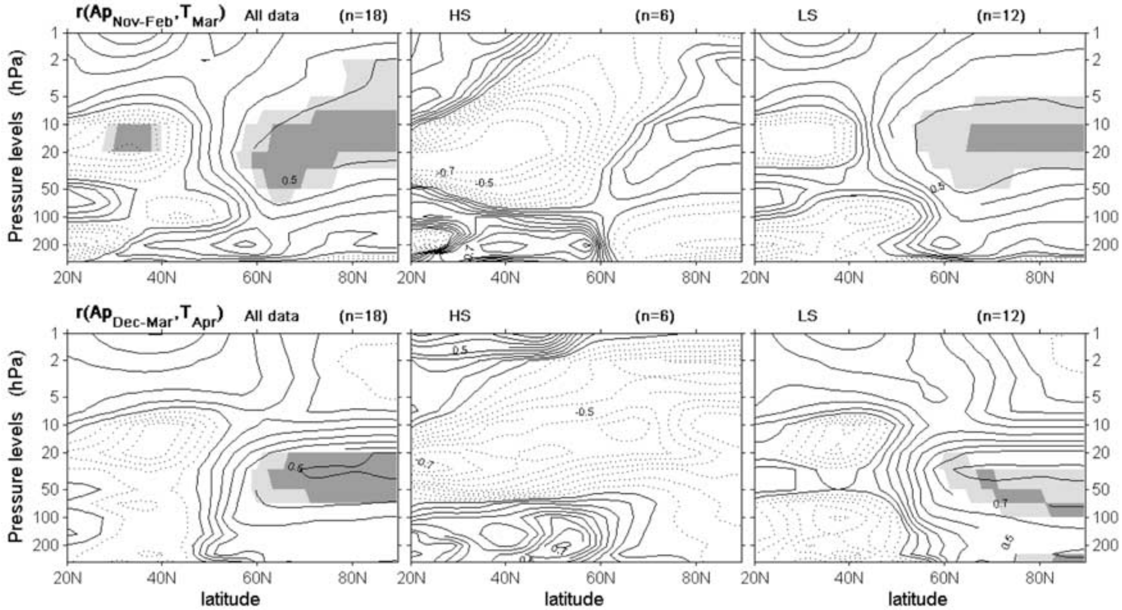

Figure 4. Same as Figure 3 but the zonal winds are replaced by the temperatures.

appear in April and May except the maximum differences have transferred down from the upper stratosphere to the middle, and then to the lower stratosphere. In May, the magnitudes of the composite differences reduce considerably. No significant differences can be found in wind and only a shallow ledge in temperature near 5–10 hPa which shows ~2 K decrease. From March to May, the upper stratosphere (>10 hPa) is generally warmer under HG than under LG. The primary feature of geomagnetic A_p signals we see in extratropical stratospheric temperatures is a descent of alternating warming and cooling cells through the winter and spring. In spring, we see a dominant warming cell descending with a cooling cell above.

4.1.1. Possible Modulation by the 11-yr SC

[22] A similar spatial pattern of the A_p signals can also be produced using linear correlations. Figure 3 shows the correlation between A_p and zonal wind and Figure 4 shows the same but between A_p and temperature for March (upper panels) and April (lower panels), where A_p is equal to the November–February, December–March mean Ap index, respectively. The 1st column shows the case when the data for the years in which no major SSW occurred during January–March were included and the 2nd and 3rd columns separate those years into HS and LS conditions, respectively. The label on the top of the panels shows the number of samples (i.e., n years) used for each condition. The correlation patterns shown in the 1st column of Figure 3 and the 1st column of Figure 4 resemble those of Figures 2a, 2c and Figures 2b, 2d, respectively. The linear correlation results imply that, if the A_p signals in zonal wind and temperature are physically real, these mid- and high latitude responses to geomagnetic forcing are likely to be linear. Figures 3 and 4 also suggest that the same correlation patterns are maintained for both wind and temperature under LS but fail to hold under HS.

[23] We have tested the robustness of the A_p signals shown in Figures 2–4 by changing the time lag by 1–2 months between A_p and the atmospheric variables, or/and by subsampling the data randomly. Similar spatial patterns emerge in the Arctic stratosphere though the absolute values of composite differences and correlation coefficients alter. When those years in which major SSWs occurred were included, similar spatial patterns can be produced, though the magnitudes of the composite differences reduce and the patterns are not significant. Both composite and correlation analyses suggest that a warmer rather than cooler upper middle Arctic stratosphere is more likely to be associated with HG from March to April in the NH, while apparent cooling of the upper stratosphere appears only in May. Possible contamination due to the 11-yr SC signals can be ruled out, as the A_p signals are preferably associated with LS rather than HS. It can also be shown that a very low positive correlation exists between A_p and F10.7 ($r \approx 0.3$) in the NH spring months (March–April) during 1958–2006.

[24] To examine more closely if the 11-yr SC does modulate the A_p signals, we have analyzed the data using scatter plots for a few selected locations. Results for a few representative locations (i.e., locations of highest correlation) are shown in Figures 5 and 6. For each of these locations, similar statistics can be obtained if the time series are extracted from a nearby locations within a radius of ~20° in latitude and ~10 km in altitude. Figure 5 shows that, when all the years are included, no significant correlation between $A_{p\ \mathrm{Nov-Feb}}$ and March zonal wind at 55°N, 5 hPa and between $A_{p\ \mathrm{Nov-Feb}}$ and March temperature at 65°N, 20 hPa can be established (Figures 5a and 5d). Note that, for the upper to mid-stratospheric polar region, in March, approximately the same zonal wind speeds and temperatures were found in the Arctic upper stratosphere in 2004 and 2006, and that they were among only a few extremely cold years since 1958. In both years, substantial

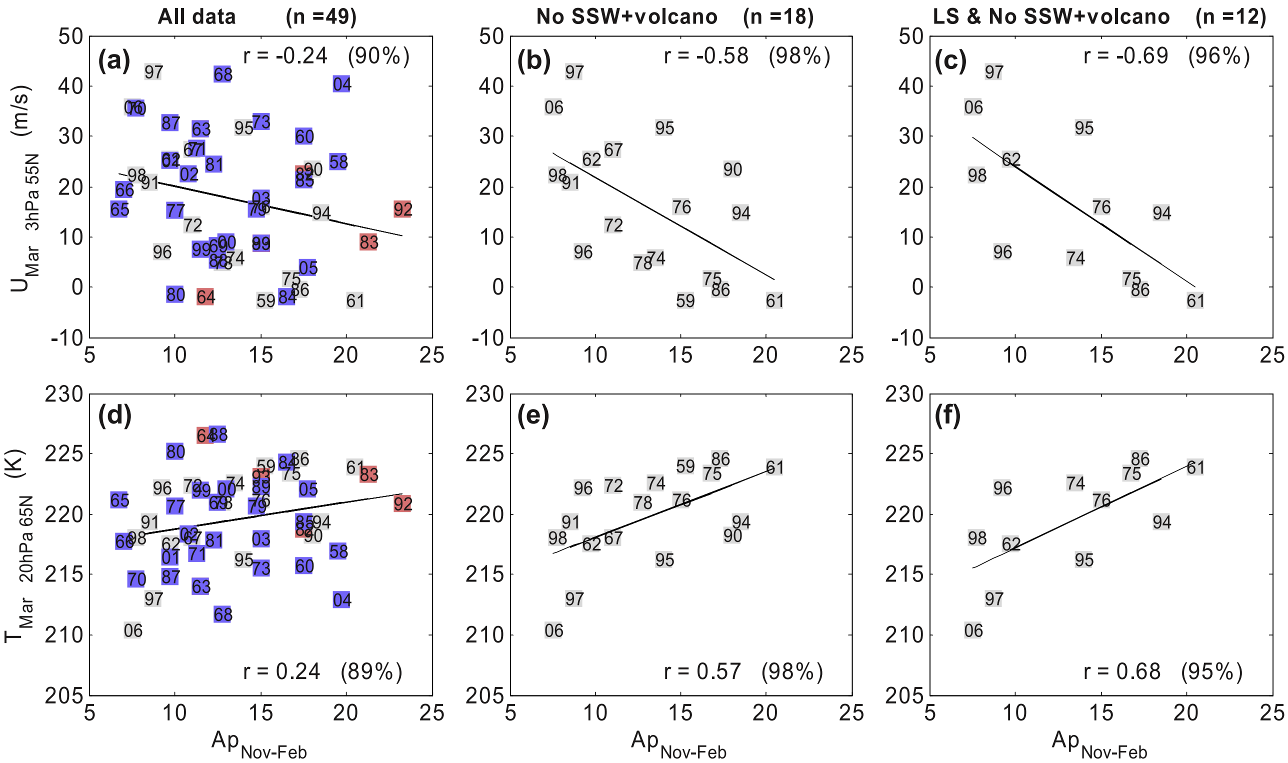

Figure 5. (a) Scatter plot of the correlation between $A_{p\ \mathrm{Nov-Feb}}$ and March zonal-mean zonal wind at 55°N, 3 hPa for all years from 1958 to 2006. All the data are shown in actual years with two-digital numbering, and a solid line shows the linear regression to the data. The years in which major SSWs occurred in January to March and the years affected by major volcanic eruption are highlighted in blue and red, respectively; (b) is the same as (a) but years affected by major SSWs and volcanic eruption are excluded; (c) is the same as (b) but only applies for those years with lower solar activity; (d), (e) and (f) are the same as (a), (b) and (c) except that the zonal-mean zonal wind is replaced by March temperature at 65°N, 20 hPa. Correlation coefficient and confidence level (in brackets) are given on the top of each panel.

descent of EPP-NO_x were observed in late winter and spring [*Randall et al.*, 2005, 2006]. The value of $A_{p\ \mathrm{Nov-Feb}}$ for 2004 is however considerably higher than that of 2006. It suggests that either A_p is not representative of all of the NO_x production, or the anomalous dynamical conditions overwhelmed *in situ* photochemistry for those extremely cold years.

[25] When the years, in which the data were affected by either the major volcanic eruptions or major SSWs are removed, the correlations become statistically significant at >95% confidence levels and the absolute values of correlation ($|r|$) increase from $\leq$0.3 to >0.55 for both wind and temperature (Figures 5b and 5e). Confirming the results shown in Figures 2–4, the upper stratospheric polar wind decreases with increasing $A_{p\ \mathrm{Nov-Feb}}$, while the middle stratospheric temperature increases. When the high solar years are removed (Figures 5c and 5f), marginal improvements in correlations are accompanied by a slight reduction in confidence levels. Figure 6 shows similar relations between $A_{p\ \mathrm{Dec-Mar}}$ and April zonal wind at 55°N, 10 hPa and between $A_{p\ \mathrm{Dec-Mar}}$ and April temperature at 65°N, 30 hPa. Data for 1990 appears to be a noticeable outlier for the case when the years, in which the data were affected by either the major volcanic eruptions or major SSWs, are removed (Figures 6b and 6d). When the high solar years are removed (Figures 5c and 5f), the absolute values of the correlation coefficients are improved to >0.8 and the improvement is achieved mainly by the filtering out of a single year, 1990. Thus a direct modulating effect by the 11-yr SC on the spring A_p signals is not established for the NH data. However an indirect modulating effect by the 11-yr SC may exist. An interesting feature worth noting is that the sampling ratio between HS and LS is 6:12, implying the polar vortex is more likely to remain stable under LS than under HS. This is consistent with the pioneer work of *Labitzke and van Loon* [1988] and *Labitzke* [2005], who found that there were more major SSWs occurring under HS. Thus the Arctic stratosphere is more likely to respond to the 11-yr SC in February [*Labitzke*, 2004] and to geomagnetic A_p in March and April.

[26] The same analyses were also undertaken for winter months from December to February with 1–3 month lags between the 4-month averaged Ap index and atmospheric zonal winds (and temperature). Few coherent A_p signals were found, except the region above 10 hPa tends to be statistically warmer in February (not shown). The lack of A_p signals in mid-winter is probably due to the fact that geomagnetic perturbations, either caused by EPP-NO_x or

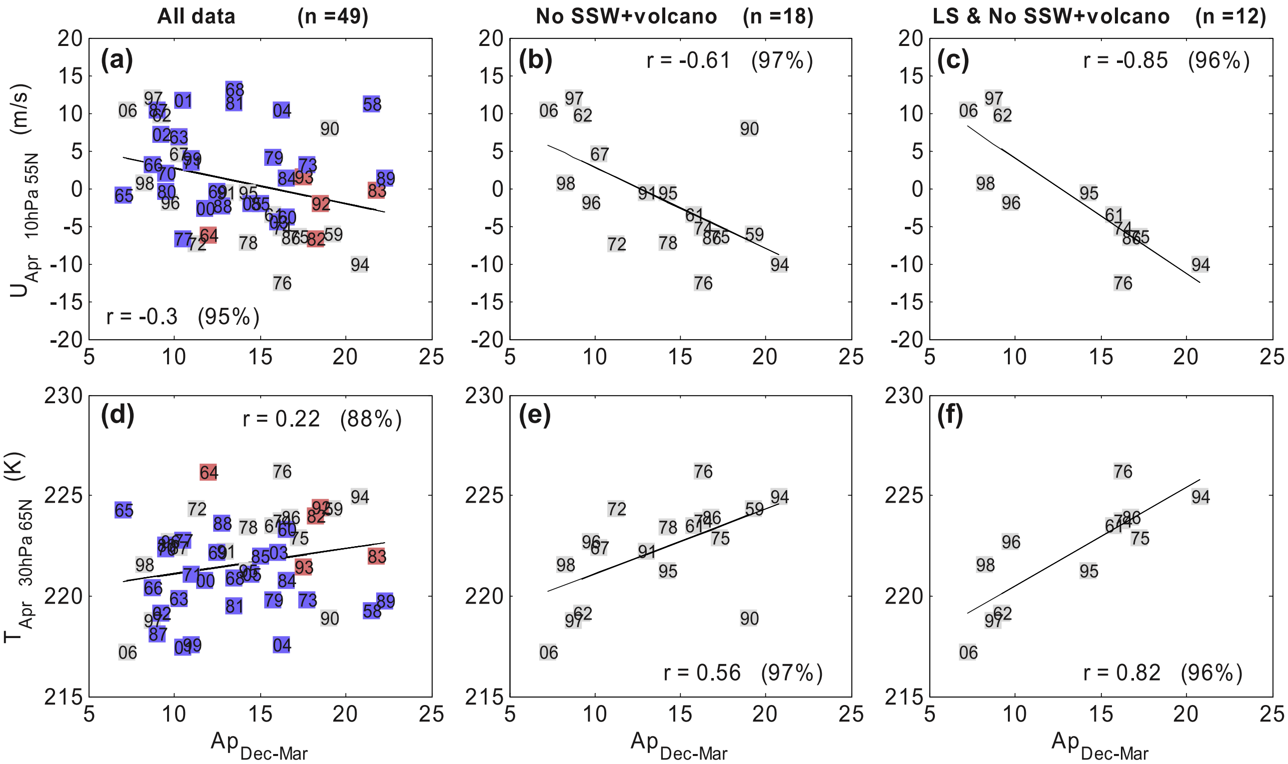

Figure 6. Same as Figure 5 except that A_p is December–March mean and zonal wind and temperature are replaced by April mean values at 55°N, 10 hPa and at 65°N, 30 hPa, respectively.

through dynamic forcing, have not yet taken effect in the stratosphere. It is also likely that geomagnetic perturbations are overpowered by the dominant effects of other processes such as the stratospheric equatorial quasi-biennial oscillation (QBO) in early winter [*Holton and Tan*, 1980; *Lu et al.*, 2008], and the 11-yr SC in late winter [*Labitzke*, 2005].

4.1.2. Possible Modulation by the QBO

[27] Linear correlations were performed to investigate whether the observed A_p signals are also modulated by the QBO. We extract the equatorial (0.56°N) zonal winds at a range of pressure levels from 10 hPa to 50 hPa from the combined ERA-40 and Operational records. The westerly and easterly phases were defined as the deseasonalized monthly zonal-mean zonal wind $\geq$2 m s^{-1} and $\leq\sim$2 m s^{-1}, and are hereinafter respectively referred to as wQBO and eQBO. In the NH, we did not find large-scale robust A_p signals in both zonal wind and temperature, except for May and when the 50 hPa deseasonalized equatorial zonal wind is used to present the QBO.

[28] Figure 7 shows linear correlations between $A_{p\ \mathrm{Jan-Apr}}$ and May zonal wind (upper panels) and between $A_{p\ \mathrm{Jan-Apr}}$ and May temperature (lower panels). The data included in the analysis are those years in which no major SSWs occurred in late winter (i.e., in February–March) and no major volcanic eruption had occurred in the past 2 years. The plots in Figure 7 indicate that, when the data are not grouped by the phases of the QBO, there is little or no correlation between $A_{p\ \mathrm{Jan-Apr}}$ and the zonal wind and between $A_{p\ \mathrm{Jan-Apr}}$ and the temperature in the extratropical stratosphere (r = ±0.2). Apart from a small region near the equator and at low altitude, where the correlation between $A_{p\ \mathrm{Jan-Apr}}$ and the zonal wind is 0.4 with confidence levels above 95%.

[29] The middle and right-most panels of Figure 7 show the same as the left panels but the data are grouped according to wQBO and eQBO phases. Under wQBO, positive $A_{p\ \mathrm{Jan-Apr}}$ signals in zonal wind are shown in a large region of the stratospheric extratropics, where $r \geq 0.8$ can be found. These $A_{p\ \mathrm{Jan-Apr}}$ signals in zonal-mean zonal winds under wQBO are highly significant with confidence levels above 99%. The mid-latitude NH polar temperature is negatively correlated with $A_{p\ \mathrm{Jan-Apr}}$ under wQBO, implying a colder NH polar region when $A_{p\ \mathrm{Jan-Apr}}$ is high. Under eQBO, no $A_{p\ \mathrm{Jan-Apr}}$ signals can be found except an oscillating positive–negative correlation pattern in the zonal wind from the sub-tropical to mid-latitudes, associated with an cold region in the sub-tropical mid-stratosphere covering 20°–45°N, and 100–10 hPa (18–32 km altitudes), which are rather stable and become statistically significant at confidence levels of 95% when the volcanic eruption effected years were excluded but major SSWs years were included (not shown).

[30] The scatter plots for those locations with peak correlations for wind and temperature under wQBO (see 2nd column of Figure 7) are shown in Figure 8, in which only the volcanic eruption affected years were excluded. Figure 8a shows that the upper stratospheric polar wind increases with increasing $A_{p\ \mathrm{Jan-Apr}}$, while Figure 8c shows that the temperature decreases with increasing $A_{p\ \mathrm{Jan-Apr}}$ under wQBO. The magnitude of the changes in wind anomaly is up to 15 m s^{-1}, and the corresponding decrease in temperature is $\sim$5 K. Figures 8b and 8d show that the

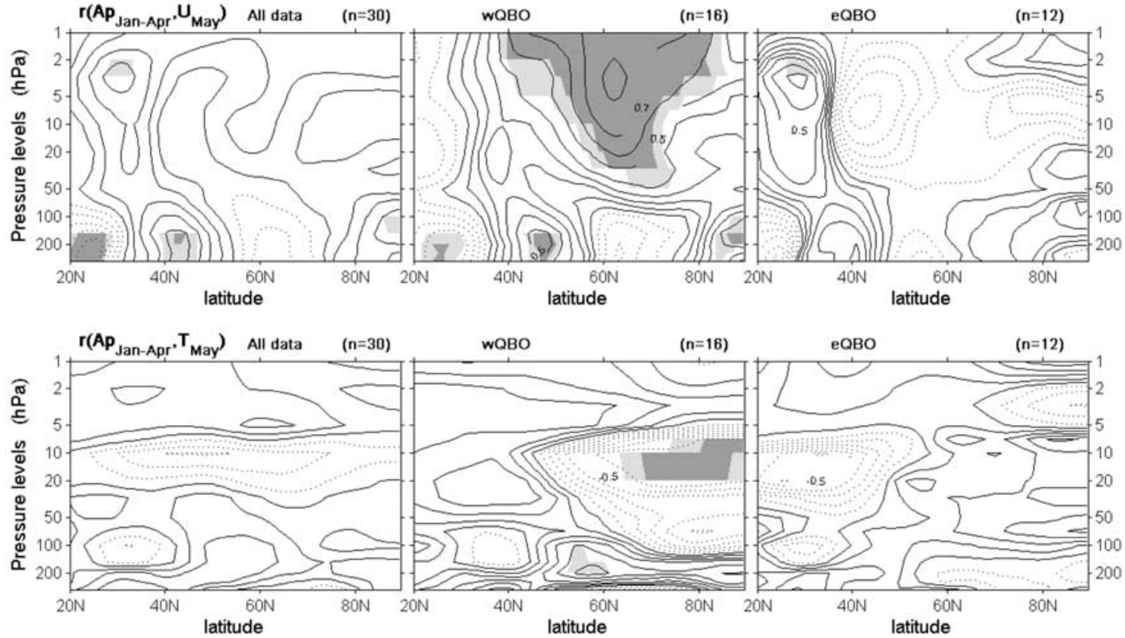

Figure 7. Correlations between $A_{p\ \mathrm{Jan-Apr}}$ and May zonal-mean zonal wind (1st row) and May temperature (2nd row) for all data (1st column), when the QBO is westerly (2nd column), and when the QBO is easterly (3rd column), displayed in the NH extratropical meridional–vertical cross section. The QBO phases are defined by May zonal-mean zonal wind anomalies at 0.56°N, 50 hPa. The contours and shadings are the same as those in Figure 3.

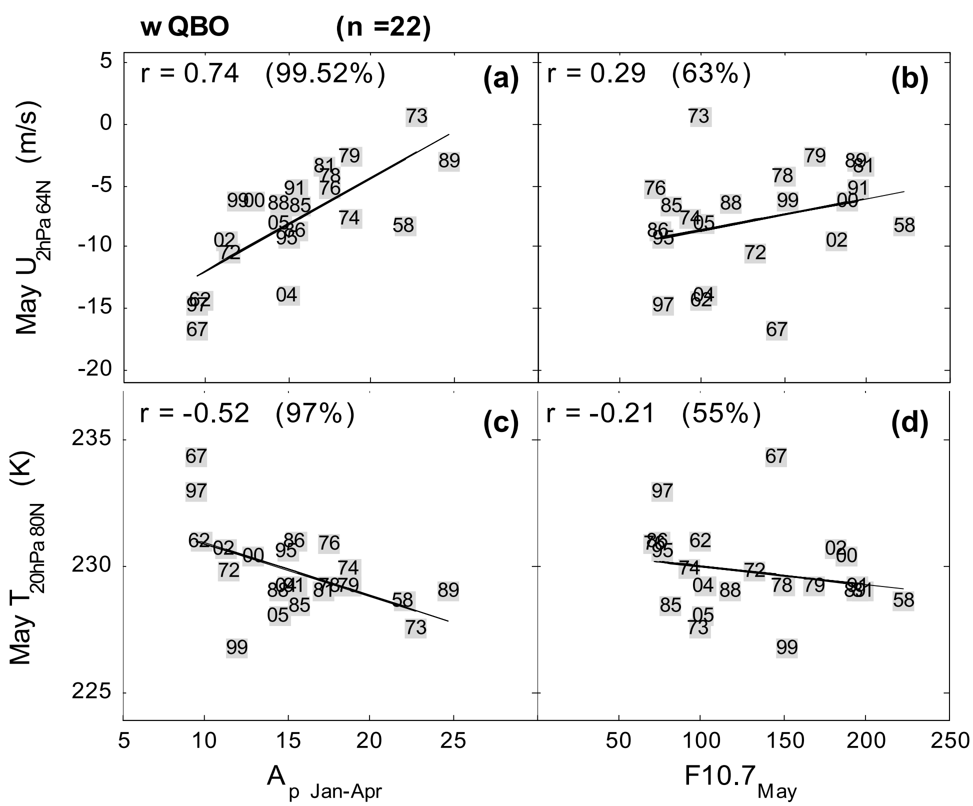

Figure 8. Scatter plots of correlations between the zonal-mean zonal wind at 64°N, 2 hPa and $A_{p\ \mathrm{Jan-Apr}}$ (a) and May F10.7 fluxes (b) under wQBO. (c) and (d) are the same as (a) and (b) but for the zonal-mean temperature at 80°N, 20 hPa. The data are shown in actual years with two-digital numbering with a solid line showing the linear regression to the data. Correlation coefficient and confidence level (in bracket) are shown on the top of each panel.

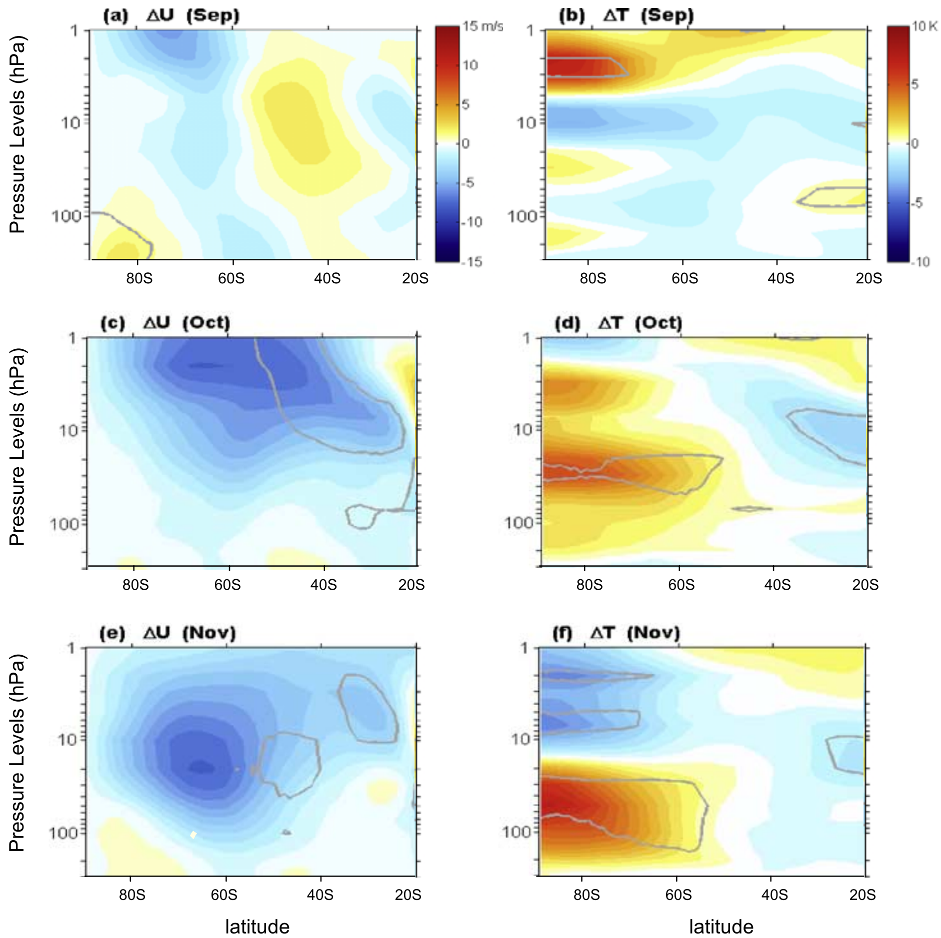

Figure 9. Same as Figure 2 but displayed in the SH meridional-vertical cross section and for the months from September to November (top to bottom). Again, the years in which a major SSW occurred or affected by a major volcanic eruption (i.e., 2002) are excluded and the data have been grouped by $\geq$ and $<$ median($A_{p\ \mathrm{May-Aug}}$).

correlations between both the wind and temperature and the proxy of the 11-yr SC, F10.7 in May, are rather weak.

4.2. A_p Signals in the SH

[31] Similar analyses were carried out for the SH but only using data after 1978. Figure 9 shows composite differences of zonal wind (left panels) and temperature (right panels) from September to November (from top to bottom) between high and low $A_{p\ \mathrm{May-Aug}}$, which is determined by its May–August median value. Similar results were obtained if a Jun–Sep median value A_p is used. Since September 1978, when data for the vortex break-up year 2002 and volcanic eruption affected years are removed, there were 12 winters under either HG or LG. Figure 9 shows easterly anomalies start in September and gradually descend to the lower stratosphere by November (Figures 9a, 9c, and 9e) which is similar to that found in the NH spring. There is a significant warming cell associated the easterly anomalies and the warming cell also descends from the upper stratosphere (~3 hPa) in September, to the lower stratosphere (~30 hPa) in October, and then to the lower most stratosphere (~200 hPa) in November (Figures 9b, 9d, and 9f).

[32] In terms of magnitudes, the Antarctic stratospheric winds are up to 8 m s^{-1} less westerly under HG than under LG, while the temperature is up to 5 K warmer. These values are smaller than those that were found in the NH (see Figure 2). Nevertheless, caution is needed when magnitude comparisons are made because the data records used remain relatively short. We did not observe significant cooling of the stratospheric polar region under HG except for November despite satellite observations suggesting more occurrences of the descent of NO_x in the SH polar vortex. Similar to that observed in the NH, the November cooling appears to be associated with an alternating warm/cool cell pattern that slowly descends over the late-winter and spring months. Also similar to the NH, the mid-latitude upper stratosphere is noticeably warmer under HG.

4.2.1. Possible Modulation by the 11-yr SC

[33] Figure 10 and Figure 11 show the correlations of $A_{p\ \mathrm{May-Aug}}$ with zonal-mean zonal wind and temperature for September (upper panels), October (middle panels), and November (lower panels). Similar to Figures 4 and 5 but for the SH, the 1st columns shows data for all years since September 1978, except for 2002, where the 2nd and 3rd columns separate those years into HS and LS years, respec-

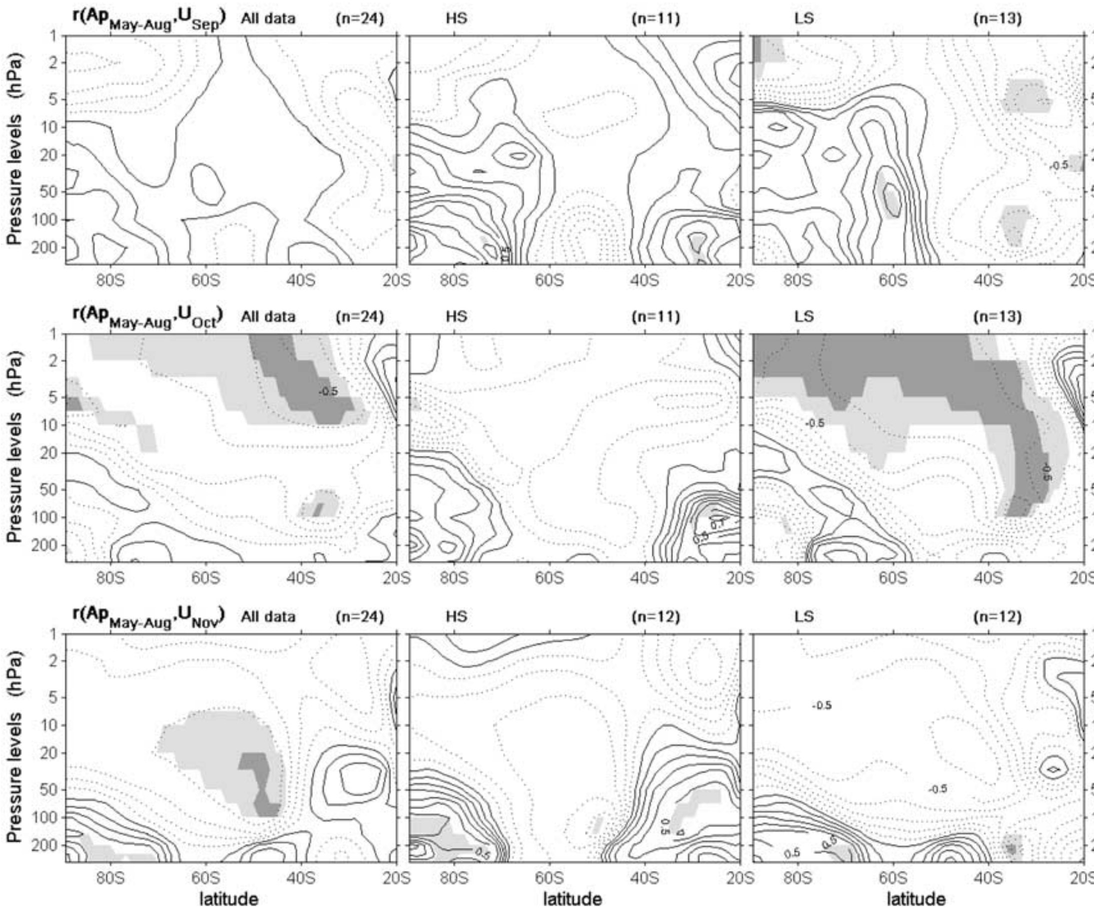

Figure 10. Same as Figure 3 but for September to November, displayed in the SH meridional–vertical cross section of 300-1 hPa and 20°–90°N.

tively. In the 1st columns, the correlation patterns for both zonal wind (Figure 10) and temperature (Figure 11) resemble those shown in Figure 9 and the correlations become statistically significant in October. In October, similar A_p signals in both wind and temperature are maintained under LS, generally with a warmer Antarctic stratosphere with negative correlations shown in the extratropics. Under HS, the correlations are no longer significant though the signs of the correlations remain the same. In September and November however the linear correlations are not significant for all three cases (all data, HS, and LS) though the signs of the correlations remain similar to those in October. For all three months, there are nearly equal amounts of data samples under HS and LS.

[34] Similar analyses were also conducted for winter months from June to August. Only localized or weak A_p signals were found. During those SH winter months, we, on the other hand, found that strong signatures of the 11-yr SC, similar to those shown in *Crooks and Gray* [2005], dominate the extratropical stratosphere (not shown). Thus, similar to the NH, it is apparent that the extratropical stratosphere responds to the 11-yr SC in middle to late winter while it responds to geomagnetic activity in spring.

[35] To examine if the 11-yr SC indeed modulates the A_p signals in the SH, the October data were analyzed using scatter plots. Figure 12 shows the correlations between $A_{p\ \mathrm{May-Aug}}$ and October stratospheric wind and temperature at two selected locations. The values of $|r|$ between $A_{p\ \mathrm{May-Aug}}$ and October zonal wind at 40°N, 5 hPa and between $A_{p\ \mathrm{May-Aug}}$ and October temperature at 65°N, 30 hPa are <0.5 when all the years since 1979 are selected (Figures 12a and 12c). When the HS years are removed (Figures 12b and 12d), significant increases in the values of $|r|$ are accompanied with marginal increases in confidence levels. Due to the marginal increases in confidence levels and the critical influence of the data point for 2003, Figure 12 does not suggest an indisputable modulation of the 11-yr SC. Note that for the period from 1979 to 2006, the $A_{p\ \mathrm{May-Aug}}$ and $\mathrm{F10.7}_{\mathrm{May-Aug}}$ are positively correlated with $r = 0.48$. Thus it is possible that the A_p signals we obtained here may be contaminated by that of the 11-yr SC. Longer data records are needed to further test if there is indeed a significant 11-yr SC modulation on atmospheric responses to geomagnetic forcing in the extratropical stratosphere.

[36] We found no significant QBO modulated $A_{p\ \mathrm{May-Aug}}$ signals for the SH late winter and spring. Apparent positive correlations were found only in zonal winds during August and September under wQBO at the altitudes around 20 hPa and 100 hPa in the Antarctic stratosphere (not shown). However these SH zonal wind correlations are only marginally significant and confined within a rather small area. It

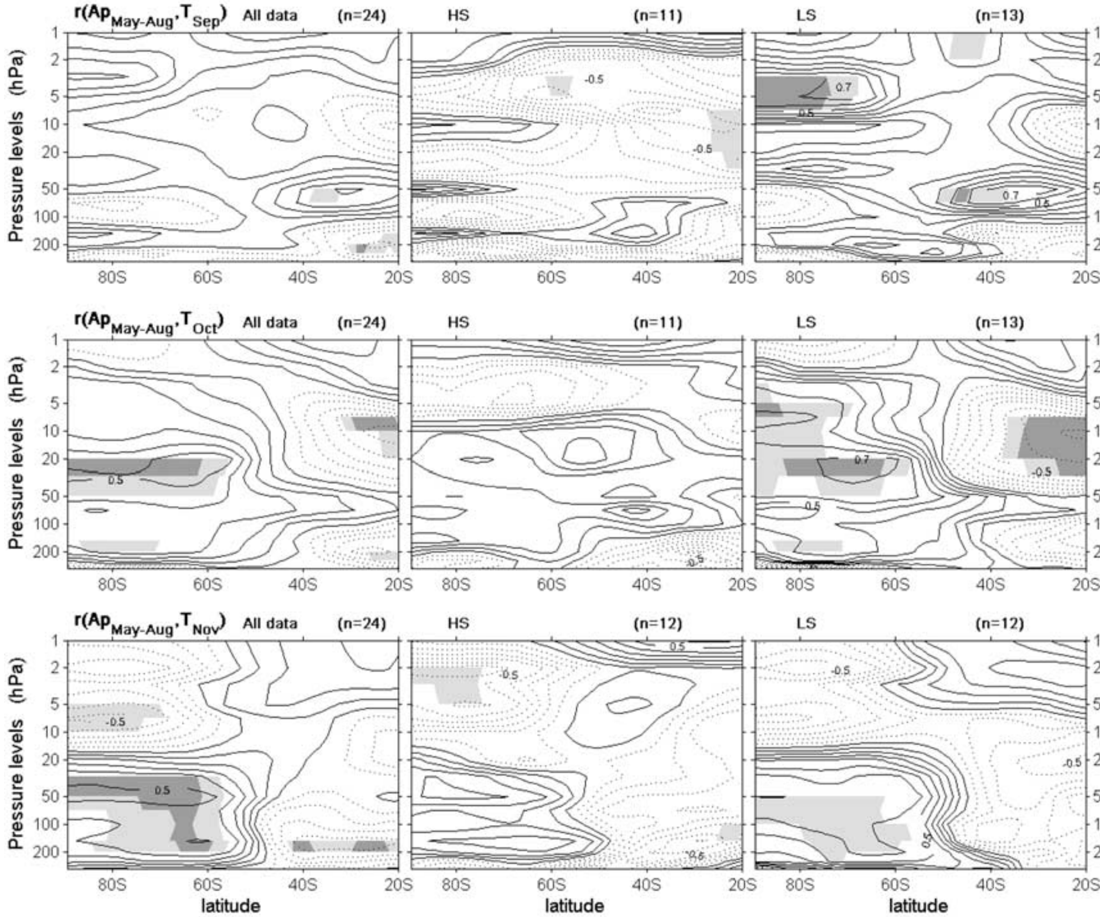

Figure 11. Same as Figure 10 but the zonal-mean zonal winds are replaced by temperature.

is likely because that the SH vortex is less dynamically disturbed and therefore less influenced by the QBO than the NH vortex that is forced by stronger planetary wave activity.

5. Discussion and Conclusions

[37] Enhancement of upper stratospheric NO_x accompanied by a simultaneous reduction in O_3 has been observed by various satellites [*Siskind et al.*, 2000; *Natarajan et al.*, 2004; *Randall et al.*, 2005; *Rinsland et al.*, 2005; *Seppälä et al.*, 2007]. Using data from the Halogen Occultation Experiment (UARS/HALOE), *Siskind and Russell* [1996] found that, in the SH, downward transport of thermospheric NO_x was a regular feature of the winter high-latitude mesosphere and the enhancements of NO_x were seen as low as 35 km. The average SH stratospheric NO_x column density with an altitude range of 23–32 km during May–August, 1991–1996 were found to be correlated with the 4-month averaged geomagnetic Ap index, implying a geomagnetic origin of EPP-NO_x [*Siskind et al.*, 2000]. However the enhancements did not seem to persist until spring when the O_3 depletion would be more efficient. Using solar occultation (SO) data from 1992 to 2005, *Randall et al.* [2007] estimate that NO_x descended from the thermosphere and the upper mesosphere contributed up to 40% of the annual SH polar stratospheric NO_x, and the interannual variability of the SH polar stratospheric NO_x is strongly correlated with low and medium energy EPP fluxes.

[38] Until the winter of 2003/2004 however the SO data sets used to investigate long-term EPP impacts showed little evidence of descending EPP-NO_x in the NH compared with the SH. The unprecedented event of descending NO_x in late winter to spring of 2003/2004 was explained as a result of an accumulative effect of low to medium energy EPP together with an exceptionally strong late winter polar vortex [*Orsolini et al.*, 2005; *Randall et al.*, 2005; *Clilverd et al.*, 2006]. However, in February and March 2006, a substantial polar upper stratospheric NO_x enhancement in the NH was observed by the Atmospheric Chemistry Experiment (ACE) during a period of minimal geomagnetic activity [*Randall et al.*, 2006]. NO_2 mixing ratios in the upper stratosphere were 3–6 times larger than observed previously in either the Arctic or Antarctic, apart from the extraordinary winter of 2003/2004, when the observed NO_x mixing ratio were yet an order of magnitude larger. Such observations raise the question about how significant is the effect of geomagnetic activity on the magnitude of NO_x enhancements in the stratospheric polar region in comparison with dynamical forcing [*Hauchecorne et al.*, 2007; *Siskind et al.*, 2007].

[39] To answer the three research questions raised in the introduction, we have investigated possible stratospheric responses to geomagnetic activity in late winter and spring

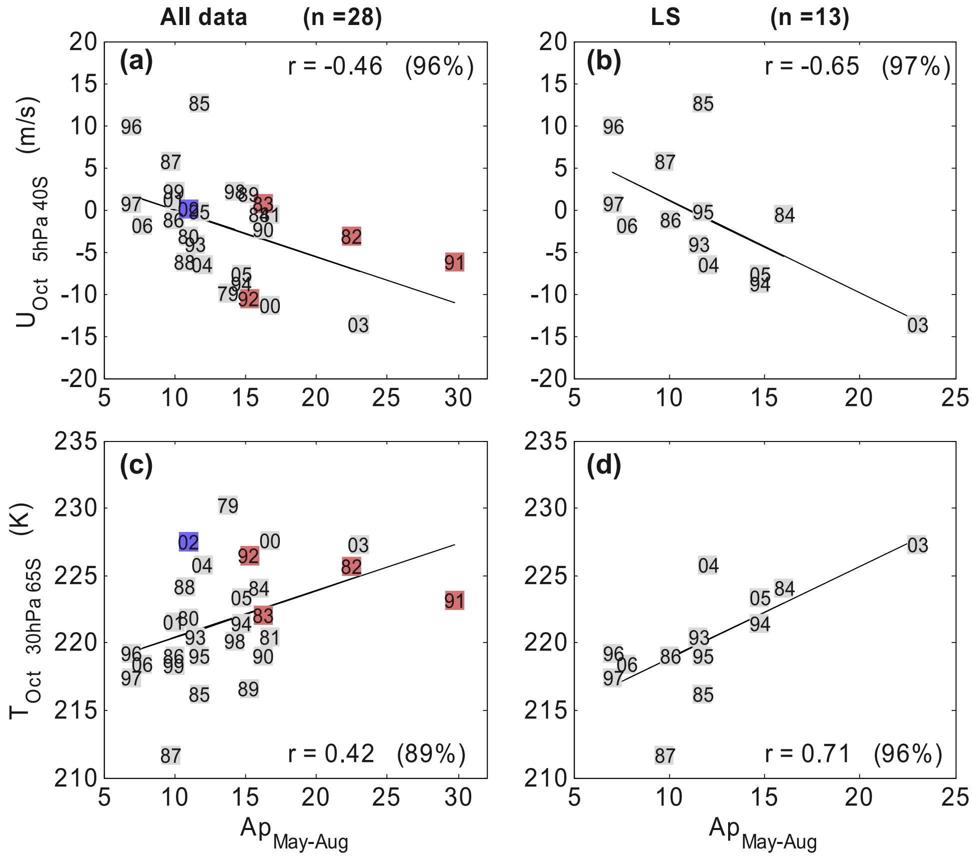

Figure 12. (a) Scatter plot of the correlation between $A_{p\ \mathrm{May-Aug}}$ and October zonal-mean zonal wind at 40°S, 5 hPa for all years since 1979 to 2006, 2002 and the years affected by the major volcanic eruption are highlighted in blue and red, respectively; (b) is the same as (a) but only for those years with lower solar activity; (c) and (d) are the same as (a) and (b) but for October temperature at 65°S, 30 hPa. Correlation coefficient and confidence level (in bracket) are given on the top of each panel.

of both hemispheres. Using the combined ERA-40 and Operational records for the periods of 1958–2006 for the NH and 1979–2006 for the SH, we have found apparently significant spring geomagnetic signals in zonal-mean zonal wind and temperature in the extratropical stratosphere. A common feature of the spring geomagnetic A_p signals in the stratospheric mid- to high latitudes is less anomalous westerly wind, and warmer polar regions, associated with higher winter time geomagnetic activity when there was a stable winter vortex. Such spring geomagnetic A_p signals are, in general, consistent with the findings of *Lu et al.* [2007], who filtered out the periods below 12 months from the radiosonde temperature data. In the spring months when the descent of EPP-NO_x may have a detectable impact, we find here that the geomagnetic A_p signals seem to descend from the upper stratosphere to the lower stratosphere. The signals become more statistically significant when the winter polar vortex is stable without major stratospheric sudden warming (SSW) occurring in middle to late winter.

[40] The spring A_p signals we have found here appear to be inconsistent with a simple local cooling effect of *in situ* chemistry between stratospheric O_3 and descending high-altitude EPP-NO_x. Firstly, the A_p signals in both wind and temperature have the opposite signs to those expected from cooling effects due to catalytic destruction of stratospheric O_3 by EPP-NO_x. Secondly, we found stronger and more significant geomagnetic signals in the NH than in the SH even though the satellite observations suggest more frequent descent of EPP-NO_x to the stratosphere in the SH. Thirdly, the observed geomagnetic A_p signals in both stratospheric wind and temperature have much larger magnitudes than would be expected from *in situ* chemical reactions alone [*Jackman et al.*, 2005, 2008]. It is however important to stress that our results here neither rule out the possibility that descending EPP-NO_x may have played a role in stratospheric circulation on an irregular basis, nor show that EPP-NO_x does not affect stratospheric ozone. Further modeling of descending EPP-NO_x and its radiative feedback is required to clarify the detailed situation.

[41] Possible modulations of the spring geomagnetic A_p signals by the 11-yr SC and the QBO were found in this study, although more data are needed to test the significance of such modulations. In spring, atmospheric responses to geomagnetic activity are preferentially clearer when solar irradiance is low. Only in the NH during May are the A_p signals found to be modulated by the QBO. The results may rule out the possibility that the detected geomagnetic signals are caused by solar UV radiative heating, but do not rule out the possibility of its relation to solar UV induced effects elsewhere in the atmosphere. The results also imply that there is a possible inter-modulating relationship among the QBO, the 11-yr SC and geomagnetic activity. The strato-

spheric polar region may respond to both solar originated perturbations through dynamical interactions. The question remains as to what mechanism is behind such modulations. A possible mechanism for the QBO modulated A_p signals might be that suggested by *Naito and Yoden* [2006], who found that poleward and downward anomalous extratropical wave forcing was associated with the wQBO, while equator-ward wave forcing was associated with the eQBO. That might point to a possible mechanism explaining why polar A_p signals are associated with the wQBO, and subtropical A_p signals are associated with the eQBO.

[42] During northern winters as well as northern summers, the 11-yr SC signal in atmospheric temperature and geopotential height have been found when subdivided according to the QBO phases [*Labitzke and van Loon*, 1988; *Salby and Callaghan*, 2006]. Similar to the 11-yr SC signals, which were found to be broadly symmetric about the equator, here we found that spring geomagnetic signatures in the extratropical stratosphere are also approximately symmetric about the equator. However such A_p signals have only been obtained by using the years when no major SSWs occurred in middle to late winter. The magnitudes of changes in spring stratospheric wind and temperatures associated with the geomagnetic A_p signals are in the range of 10–20 m s^{-1} and 5–10 K. They are comparable with those of the 11-yr SC signals typically found in late winter [*Labitzke*, 2004; *Crooks and Gray*, 2005]. Together with those previous findings, we suggest that those solar or geomagnetic signals in the extratropical stratosphere are not consistent with a direct or *in situ* consequence of radiative heating by UV–ozone interaction, or EPP-NO_x effects on ozone.

[43] We suggest that there might be an indirect chemical–dynamic connection to the stratosphere, with geomagnetic and solar far-UV perturbations in the mesosphere and the lower thermosphere, where routine production of NO_x is formed by the dissociation of N_2 by far-UV solar radiation and EPP in the auroral zone. It is likely that the geomagnetic A_p signals found in this study result from a coupling between mean flow and atmospheric waves, including planetary and gravity waves, as suggested earlier by *Arnold and Robinson* [2001]. In the stratosphere, vertically propagating planetary waves from the troposphere control the intensity of the equator-to-pole transport of O_3 by the Brewer–Dobson circulation. In the mesosphere, the interaction between gravity waves and zonal winds controls the transport strength from summer pole to winter pole. Temperature changes induced by either EPP or far-UV solar radiation in the mesosphere or the thermosphere may cause changes in vertical propagating wave ducting. It is also possible that EPP-NO_x may cause changes of mesospheric O_3, which lead to anomalous changes of the temperature gradient between the two poles, consequently altering the mesospheric pole-to-pole circulation. Such a change would modify the refraction or ducting condition of planetary and gravity waves. By either suppressing or enhancing the propagation/reflection of planetary waves into the stratospheric polar region, it leads to anomalous warming or cooling in the stratospheric polar regions. Nevertheless, the detailed mechanism that produces the spring geomagnetic signals found in this study and drives their downward propagation remains unclear. More data and modeling exercises are needed in order to answer this intriguing question, as our statistical analyses have not been able to provide an unequivocal answer to it.

[44] **Acknowledgments.** We would like to thank Martin J. Jarvis for his useful discussions and guidance. The SAGE III data were obtained from the NASA Langley Research Center Atmospheric Science Data Center. We are very grateful to two anonymous referees whose comments significantly improved the paper.

References

Arnold, N. F., and T. R. Robinson (1998), Solar cycle changes to planetary wave propagation and their influence on the middle atmosphere circulation, *Ann. Geophys.*, *16*(1), 69–76.

Arnold, N. F., and T. R. Robinson (2001), Solar magnetic flux influences on the dynamics of the winter middle atmosphere, *Geophys. Res. Lett.*, *28*(12), 2381–2384.

Bertaux, J. L., E. Kyrölä, and T. Wehr (2000), Stellar occultation technique for atmospheric ozone monitoring: GOMOS on Envisat, *Earth Observ. Quart.*, *67*, 17–20.

Boberg, F., and H. Lundstedt (2002), Solar wind variations related to fluctuations of the North Atlantic Oscillation, *Geophys. Res. Lett.*, *29*(15), 1718, doi:10.1029/2002GL014903.

Boberg, F., and H. Lundstedt (2003), Solar wind electric field modulation of the NAO: A correlation analysis in the lower atmosphere, *Geophys. Res. Lett.*, *30*(15), 1825, doi:10.1029/2003GL017360.

Bochnicek, J., and P. Hejda (2005), The winter NAO pattern changes in association with solar and geomagnetic activity, *J. Atmos. Sol. Terr. Phys.*, *67*, 17–32.

Brasseur, G. P., and S. Solomon (2005), *Aeronomy of the Middle Atmosphere*, 3rd ed., Springer, Dordrecht.

Callis, L. B., R. E. Boughner, M. Natarajan, J. D. Lambeth, D. N. Baker, and J. B. Blake (1991), Ozone depletion in the high-latitude lower stratosphere-1979–1990, *J. Geophys. Res.*, *96*(D2), 2921–2937.

Callis, L. B., M. Natarajan, and J. D. Lambeth (2001), Solar-atmospheric coupling by electrons (SOLACE) 3. Comparisons of simulations and observations, 1979–1997, issues and implications, *J. Geophys. Res.*, *106*(D7), 7523–7539.

Charlton, A. J., and L. M. Polvani (2007), A new look at stratospheric sudden warmings. part I. Climatology and modelling benchmarks, *J. Clim.*, *20*, 449–469.

Clilverd, M. A., A. Seppälä, C. J. Rodger, P. T. Verronen, and N. R. Thomson (2006), Ionospheric evidence of thermosphere-to-stratosphere descent of polar NO_x, *Geophys. Res. Lett.*, *33*, L19811, doi:10.1029/2006GL026727.

Crooks, S. A., and L. J. Gray (2005), Characterization of the 11-year solar signal using a multiple regression analysis of the ERA-40 dataset, *J. Clim.*, *18*(7), 996–1015.

Davis, R. E. (1976), Predictability of sea surface temperature and sea level pressure anomalies over the North Pacific Ocean, *J. Phys. Oceangr.*, *6*, 249–266.

Garrett, H. B., A. J. Dessler, and T. W. Hill (1974), I. Influence of solar wind variability on geomagnetic activity, *J. Geophys. Res.*, *79*(31), 4603–4610.

Hauchecorne, A., et al. (2005), First simultaneous global measurements of nighttime stratospheric NO_2 and NO_3 observed by global ozone monitoring by Occultation of Stars (GOMOS)/Envisat in 2003, *J. Geophys. Res.*, *110*, D18301, doi:10.1029/2004JD005711.

Hauchecorne, A., J.-L. Bertaux, F. Dalaudier, J. M. Russell, M. G. Mlynczak, E. Kyrölä, and D. Fussen (2007), Large increase of NO_2 in the north polar mesosphere in January–February 2004: Evidence of a dynamical origin from GOMOS/ENVISAT and SABER/TIMED data, *Geophys. Res. Lett.*, *34*, L03810, doi:10.1029/2006GL027628.

Holton, J. R., and H. C. Tan (1980), The influence of the equatorial quasi-biennial oscillation on the global circulation at 50 mb, *J. Atmos. Sci.*, *37*, 2200–2208.

Jackman, C. H., and R. D. McPeters (2004), The effect of solar proton events on ozone and other constituents, in *Solar Variability and Its Effect on the Earth's Atmosphere and Climate System*, edited by J. Pap et al., AGU Monogr. Ser., Washington D. C.

Jackman, C. H., M. T. DeLand, G. J. Labow, E. L. Fleming, D. K. Weisenstein, M. K. W. Ko, M. Sinnhuber, and J. M. Russell III (2005), Neutral atmospheric influences of the solar proton events in October–November 2003, *J. Geophys. Res.*, *110*, A09S27, doi:10.1029/2004JA010888.

Jackman, C. H., R. G. Roble, and E. L. Fleming (2007), Mesospheric dynamical changes induced by the solar proton events in October–November 2003, *Geophys. Res. Lett.*, *34*, L04812, doi:10.1029/2006GL028328.

Jackman, C. H., et al. (2008), Short- and medium-term atmospheric effects of very large solar proton events, *Atmos. Chem. Phys.*, *8*, 765–785.

Kyrölä, E., et al. (2004), GOMOS on Envisat: An overview, *Adv. Space Res.*, *33*, 1020–1028.

Labitzke, K. (2004), On the signal of the 11-year sunspot cycle in the stratosphere and its modulation by the quasi-biennial oscillation, *J. Atmos. Sol. Terr. Phys.*, *66*(13–14), 1151–1157.

Labitzke, K. (2005), On the solar cycle-QBO relationship: A summary, *J. Atmos. Sol. Terr. Phys.*, *67*(1–2), 45–54.

Labitzke, K., and H. van Loon (1988), Associations between the 11-year solar-cycle, the QBO and the atmosphere 1. The troposphere and stratosphere in the Northern Hemisphere in winter, *J. Atmos. Terr. Phys.*, *50*(3), 197–206.

Labitzke, K., and H. van Loon (2000), The QBO effect on the solar signal in the global stratosphere in the winter of the Northern Hemisphere, *J. Atmos. Sol. Terr. Phys.*, *62*(8), 621–628.

Langematz, U., J. L. Grenfell, K. Matthes, P. Mieth, M. Kunze, B. Steil, and C. Brühl (2005), Chemical effects in 11-year solar cycle simulations with the Freie Universität Berlin Climate Middle Atmosphere Model with online chemistry (FUB-CMAM-CHEM), *Geophys. Res. Lett.*, *32*, L13803, doi:10.1029/2005GL022686.

Lu, H., M. J. Jarvis, H. F. Graf, P. C. Young, and R. B. Horne (2007), Atmospheric temperature response to solar irradiance and geomagnetic activity, *J. Geophys. Res.*, *112*, D11109, doi:10.1029/2006JD007864.

Lu, H., M. Bladwin, L. Gray, and M. J. Jarvis (2008), Decadal-scale changes in the effect of the QBO on the northern stratospheric polar vortex, *J. Geophys. Res.*, *113*, D10114, doi:10.1029/2007JD009647.

Marsh, D. R., R. R. Garcia, D. E. Kinnison, B. A. Boville, F. Sassi, S. C. Solomon, and K. Matthes (2007), Modeling the whole atmosphere response to solar cycle changes in radiative and geomagnetic forcing, *J. Geophys. Res.*, *112*, D23306, doi:10.1029/2006JD008306.

Mayaud, P. N. (1980), *Derivation, Meaning, and Use of Geomagnetic Indices*, AGU, Washington, D. C.

Naito, Y., and S. Yoden (2006), Behavior of planetary waves before and after stratospheric sudden warming events in several phases of the equatorial QBO, *J. Atmos. Sci.*, *63*(6), 1637–1649.

Natarajan, M., E. E. Remsberg, L. E. Deaver, and J. M. Russell III (2004), Anomalously high levels of NO_x in the polar upper stratosphere during April, 2004: Photochemical consistency of HALOE observations, *Geophys. Res. Lett.*, *31*, L15113, doi:10.1029/2004GL020566.

Orsolini, Y. J., G. L. Manney, M. L. Santee, and C. E. Randall (2005), An upper stratospheric layer of enhanced HNO_3 following exceptional solar storms, *Geophys. Res. Lett.*, *32*, L12S01, doi:10.1029/2004GL021588.

Randall, C. E., et al. (2002), Validation of POAM III NO_2 measurements, *J. Geophys. Res.*, *107*(D20), 8299, doi:10.1029/2001JD000471.

Randall, C. E., et al. (2005), Stratospheric effects of energetic particle precipitation in 2003–2004, *Geophys. Res. Lett.*, *32*, L05802, doi:10.1029/2004GL022003.

Randall, C. E., V. L. Harvey, C. S. Singleton, P. F. Bernath, C. D. Boone, and J. U. Kozyra (2006), Enhanced NO_x in 2006 linked to strong upper stratospheric Arctic vortex, *Geophys. Res. Lett.*, *33*, L18811, doi:10.1029/2006GL027160.

Randall, C. E., V. L. Harvey, C. S. Singleton, S. M. Bailey, P. F. Bernath, M. Codrescu, H. Nakajima, and J. M. Russell III (2007), Energetic particle precipitation effects on the Southern Hemisphere stratosphere in 1992–2005, *J. Geophys. Res.*, *112*, D08308, doi:10.1029/2006JD007696.

Rinsland, C. P., C. Boone, R. Nassar, K. Walker, P. Bernath, J. C. McConnell, and L. Chiou (2005), Atmospheric Chemistry Experiment (ACE) Arctic stratospheric measurements of NO_x during February and March 2004: Impact of intense solar flares, *Geophys. Res. Lett.*, *32*, L16S05, doi:10.1029/2005GL022425.

Rozanov, E., L. Callis, M. Schlesinger, F. Yang, N. Andronova, and V. Zubov (2005), Atmospheric response to NO_y source due to energetic electron precipitation, *Geophys. Res. Lett.*, *32*, L14811, doi:10.1029/2005GL023041.

Salby, M. L., and P. F. Callaghan (2006), Relationship of the quasi-biennial oscillation to the stratospheric signature of the solar cycle, *J. Geophys. Res.*, *111*, D06110, doi:10.1029/2005JD006012.

Seppälä, A., P. T. Verronen, E. Kyrölä, S. Hassinen, L. Backman, A. Hauchecorne, J. L. Bertaux, and D. Fussen (2004), Solar proton events of October–November 2003: Ozone depletion in the Northern Hemisphere polar winter as seen by GOMOS/Envisat, *Geophys. Res. Lett.*, *31*, L19107, doi:10.1029/2004GL021042.

Seppälä, A., P. T. Verronen, M. A. Clilverd, C. E. Randall, J. Tamminen, V. Sofieva, L. Backman, and E. Kyrölä (2007), Arctic and Antarctic polar winter NO_x and energetic particle precipitation in 2002–2006, *Geophys. Res. Lett.*, *34*, L12810, doi:10.1029/2007GL029733.

Siskind, D. E. (2000), On the coupling between the middle and upper atmospheric odd nitrogen, in *Atmospheric Science Across the Stratopause*, *Geophys. Monogr. Ser.*, vol. 123, pp. 101–116, AGU, Washington, D. C.

Siskind, D. E., and J. M. Russell III (1996), Coupling between middle and upper atmospheric NO: Constraints from HALOE observations, *Geophys. Res. Lett.*, *23*(2), 137–140.

Siskind, D. E., G. E. Nedoluha, C. E. Randall, M. Fromm, and J. M. Russell (2000), An assessment of Southern Hemisphere stratospheric NO_x enhancements due to transport from the upper atmosphere, *Geophys. Res. Lett.*, *27*(3), 329–332.

Siskind, D. E., S. D. Eckermann, L. Coy, J. P. McCormack, and C. E. Randall (2007), On recent interannual variability of the Arctic winter mesosphere: Implications for tracer descent, *Geophys. Res. Lett.*, *34*, L09806, doi:10.1029/2007GL029293.

Solomon, S., P. J. Crutzen, and R. G. Roble (1982), Photochemical coupling between the thermosphere and the lower atmosphere: 1. Odd nitrogen from 50 to 120 km, *J. Geophys. Res.*, *87*(C9), 7206–7220.

Thejll, P., B. Christiansen, and H. Gleisner (2003), On correlations between the North Atlantic Oscillation, geopotential heights, and geomagnetic activity, *Geophys. Res. Lett.*, *30*(6), 1347, doi:10.1029/2002GL016598.

Uppala, S. M., et al. (2005), The ERA-40 reanalysis, *Q. J. R. Meteorol. Soc.*, *131*(612), 2961–3012.

Vennerstrøm, S., and E. Friis-Christensen (1996), Long-term and solar cycle variation of the ring current, *J. Geophys. Res.*, *101*(A11), 24,727–24,735.

Zubov, V., E. Rozanov, A. Shirochkov, L. N. Makarova, T. Egorova, A. Kiselev, Y. Ozolin, I. Karol, and W. Schmutz (2005), Modeling of the Joule heating influence on the circulation and ozone concentration in the middle atmosphere, *J. Atmos. Terr. Phys.*, *67*, 155–162, doi:10.1016/j.jastp.2004.07.024.

M. A. Clilverd and H. Lu, Physical Sciences Division, British Antarctic Survey, High Cross, Madingley Road, Cambridge CB3 0ET, UK. (macl@bas.ac.uk; hlu@bas.ac.uk)

L. Hood, Lunar and Planetary Laboratory, University of Arizona, Tuczon, AZ 85721, USA. (lon@lpl.arizona.edu)

A. Seppälä, Earth Observation, Finnish Meteorological Institute, P.O. Box 503, FI-00101 Helsinki, Finland. (annika.seppala@fmi.fi)